International Refereed Journal of Engineering and Science (IRJES)
ISSN (Online) 2319-183X, (Print) 2319-1821
Volume 2, Issue 2(February 2013), PP.54-80
www.irjes.com

Optimization for Spherical Phased Array Antenna

Adnan Affandi[1] , Mubashshir Husain[2] & Navin Kasim[3]

(Electrical and Computer Engineering Department, King Abdul Aziz University O BOX: 80204, Jeddah 21589)

ABSTRACT

The main feature of the phased array antenna is its ability to control the amplitude and phase excitation of each radiating source in order to form and scan the main beam by electronic control without any mechanical contributions. The phased array is composed of a group of element sources which are distributed and oriented in a linear, two or three dimensional configurations. A comprehensive computer program is developed using matlab software to perform the analysis of linear array (uniform and nonuniform amplitude), planar array, circular array and spherical array to draw the field patterns for the different versions of phased array antennas. The basic parameters of the phased array antenna are calculated and analyses to discuss their effects on beam shaping. Spherical phased array has been developed as three dimensional configurations to perform and enhance maximum beam steering. The general equation for spherical phased array (SPA) antenna is derived. The program GPA–2D can draw the array factor in 2- Dimension with respect to linear (uniform and nonuniform amplitude), planner, circular and spherical phased array antennas. However, the program GPA–3D can draw the array factor in 3- Dimension with respect to planar, circular and spherical phased array antennas. Analysis of developed spherical phased array antenna and optimization technique is performed to enhance beam steering capabilities to get the optimized results for 5-sections and 7-sections of SPA antenna (Broad side array).

Keywords- *Phase Array Antenna, Matlab, Linear Array , Plannar Array , Circular Array, Spherical Phase Array*

1.Introduction

An antenna acts to convert guided waves on a transmission structure into free space waves. As part of a transmitting or receiving system, it is designed to radiate or receive electromagnetic waves. Phased array antennas play a major role in the recent and future advanced radars and communication systems [1].

Basically, the phased array is composed of a group of element sources which are distributed and oriented in a linear, two or

three dimensional configurations. The main feature of the phased array antenna is its ability to control the amplitude and phase excitation of each radiating source in order to form and scan the main beam by electronic control without any mechanical contributions [2].

The total field of the array is determined by the vector addition of all fields radiated by the individual elements. To provide very directive patterns, it is necessary for these fields to interfere constructively (add) in the desired direction and

Interfere destructively (cancel each other) in the remaining space.

We introduce the parameters that characterize the antennas and then array elements and feeding Structures for Phased Arrays [5]. The basic parameters of the phased array antenna are the array factor, radiation pattern, directivity, beam width and impedance [2]. These parameters can be controlled by a number of controls that can be used to shape the overall pattern of the antenna. These parameters are the geometrical configuration of the overall array (linear, planar, circular, and spherical), the relative displacement between the element sources, the excitation amplitude of the individual elements, the excitation phase shift of the individual elements, and the relative pattern of the individual elements.

To simplify the presentation and give a better physical interpretation of the techniques, a two-element array has first been considered and Pattern Multiplication takes place. The analysis of uniform and nonuniform linear arrays with any desired number of elements is discussed with maximum radiation that can be oriented in any direction to form a scanning array [3].

In addition to placing elements along a line (to form a linear array), individual radiators can be positioned along a rectangular grid to form a rectangular or planar array [3]. Planar arrays provide additional variables which can be used to control and shape the pattern of the array. Planar arrays are more versatile and can provide more

symmetrical patterns with lower side lobes. In addition, they can be used to scan the main beam of the antenna towards any point in space.

The spherical phased array antenna (SPA) is designed to operate in microwave range in order to maximize beam steering [4]. The spherical phased Array antenna is composed of identical feeding sources distributed over the surface of a sphere. Proposed spherical array model is adopted using the Array Factor equation $AF(\theta,\phi)$ for general spherical phased array antennas, where it can be segmented into many sections with each one as a circular array. The general equation for spherical phased array (SPA) antenna is derived. A comprehensive computer program is developed using matlab software to perform the analysis for different phased array configurations such as linear array (uniform and nonuniform), planar array, circular array and spherical array, including calculation and drawings of the array factor, then optimizing the spherical phased array (SPA) antenna of 5-sections and 7-sections, respectively.

1.1Antennas and phased Array antenna

In addition to receiving and transmitting energy, an antenna is usually required to direct the radiated energy in some directions and suppress it in others.

Arrays of antennas can be arranged in space and inter-connected to produce a directional radiation pattern. Such a configuration of multiple radiating elements is referred to as an ARRAY ANTENNA. Rather than increasing the size of an antenna to get more directive characteristics, we use an assembly of radiating elements in an electrical and geometrical configuration to achieve this goal.

Basically, the phased array antenna is composed of a group of individual radiators which are distributed and oriented in a linear, two or three dimensional spatial configurations. The amplitude and phase excitations of each radiator (element) can be individually controlled to form a radiated beam of specific desired shape in space. The position of the beam in space is controlled electronically by adjusting the phase of excitation signals of the individual radiators. Hence beam scanning is accomplished with the antenna structure remaining fixed in space without the involvement of mechanical motion in the scanning process.

1.2 Linear Phased Array Antenna

The total field of the array is determined by the vector addition of the fields radiated by the individual elements. This assumes that the current in each element is the same as that of the isolated element. This is usually not the case and depends on the separation between the elements. To provide very directive patterns, it is necessary that the fields from the elements of the array interfere constructively (add) in the desired directions and interfere destructively (cancel each other) in the remaining space. Ideally this can be accomplished, however practically it is only approached. In an array of identical elements, there are five controls that can be used to shape the overall pattern of the antenna. These are:

1. The geometrical configuration of the overall array (linear, circular, rectangular, spherical, etc.).
2. The relative displacement between the elements.
3. The excitation amplitude of the individual elements.
4. The excitation phase of the individual elements
5. The relative pattern of the individual elements.

1.2.1 N-Element Linear Array Uniform Amplitude and Spacing

Now the arraying of elements has been introduced and it was illustrated by the two-element array, let us generalize this method to include *N* elements. Referring to the geometry of Figure 2.2(a), let us assume that all the elements have identical amplitudes but each succeeding element has a progressive phase lead current excitation relative to the preceding one (β represents the phase by which the current in each element leads the current of the preceding element). An array of identical elements all of identical magnitude and each with a progressive phase is referred to as a uniform array. The array factor can be obtained by considering the elements to be point sources. If the actual elements are not isotropic sources, the total field can be formed by multiplying the array factor of the isotropic sources by the field of n single element. This is the pattern multiplication rule of equation (1.5), and it applies only for arrays of identical elements.

E(total) = [E(single element at reference point)] × [array factor]
(1.5)

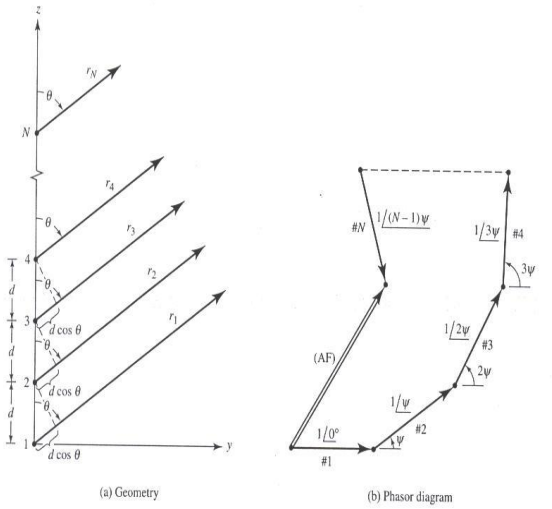

Figure 2.2, Far-field geometry and phasor diagram of N-element array of isotropic sources positioned along the z-axis
The array factor is given by

$$A_F = 1 + e^{+j(kd\cos\theta+\beta)} + e^{j2(kd\cos\theta+\beta)} + ... + e^{j(N-1)(kd\cos\theta+\beta)} \quad A_F = \sum_{n=1}^{N} e^{+j(n-1)(kd\cos\theta+\beta)} \tag{1.6}$$

which can be written as [3],

$$A_F = \sum_{n=1}^{N} e^{j(n-1)\psi} \tag{1-7a}$$

$$where\, \psi = kd\cos\theta + \beta \tag{1-7b}$$

Since the total array factor for the uniform array is a summation of exponentials, it can be represented by the vector sum of N phasors each of unit amplitude and progressive phase φ relative to the previous one. Graphically this is illustrated by the phasor diagram in Figure 2.2(b). It is apparent from the phasor diagram that the amplitude and phase of the AF can be controlled in uniform arrays by properly selecting the relative phase φ between the elements; in nonuniform arrays, the amplitude as well as the phase can be used to control the formation and distribution of the total array factor. The array factor of (1-7a) can also be expressed in an alternate, compact and closed form whose functions and their distributions are more recognizable. This is accomplished as follows: Multiplying both sides of (1-7) by $e^{j\varphi}$, it can be written as

$$(AF)e^{j\varphi} = e^{j\psi} + e^{j2\psi} + e^{j3\psi} + ... + e^{j(N-1)\psi} + e^{jN\psi} \tag{1-8}$$

Subtracting (1-7) from (1-8) reduces to

$$AF(e^{j\psi} - 1) = (-1 + e^{jN\psi}) \tag{1-9}$$

This can also be written as [3], $AF = \left[\frac{e^{jN\psi} - 1}{e^{j\psi} - 1}\right] = e^{j[(N-1)/2]\psi}\left[\frac{e^{j(N/2)\psi} - e^{-j(N/2)\psi}}{e^{j(1/2)\psi} - e^{-j(1/2)\psi}}\right]$

$$= e^{j[(N-1)/2]\psi}\left[\frac{Sin\left(\frac{N}{2}\psi\right)}{\sin\left(\frac{1}{2}\psi\right)}\right] \quad (1\text{-}10)$$

If the reference point is the physical center of the array, the array factor of (3-10) reduces to

$$AF = \left[\frac{Sin\left(\frac{N}{2}\psi\right)}{\sin\left(\frac{1}{2}\psi\right)}\right] \quad (1\text{-}10a)$$

For small vales of ψ, the above expression can be approximated by

$$AF \approx \left[\frac{Sin\left(\frac{N}{2}\psi\right)}{\frac{\psi}{2}}\right] \quad (1\text{-}10b)$$

The maximum value of (1-10a) or (1-10b) is equal to N. To normalize the array factors so that the maximum value of each is equal to unity,

$$(AF)_n = \frac{1}{N}\left[\frac{Sin\left(\frac{N}{2}\psi\right)}{\sin\left(\frac{\psi}{2}\right)}\right] \quad (1\text{-}10c)$$

For n= N, 2N, 3N... (1-10) attains its maximum values because it reduces to a sin (0)/0 forms. The values of *n* determine the order of the nulls (first, second, etc.). For a zero to exist, the argument of the arccosine cannot exceed unity. Thus the number of nulls that can exist will be a function of the element separation *d* and the phase excitation difference β .The maximum values of (1-l0c) occur when,

$$\frac{\psi}{2} = \frac{1}{2}(kd\cos\theta + \beta)\Big|_{\theta=\theta_m} = \pm m\pi \Rightarrow \theta_m = \cos^{-1}\left[\frac{\lambda}{2\pi d}(-\beta \pm m\pi)\right]$$

$$m = 0,1,2,.... \quad (1\text{-}12)$$

The array factor of (1-l0d) has only one maximum and occurs when m=0 in (1-12). That is,

$$\theta_m = \cos^{-1}\left(\frac{\lambda\beta}{2\pi d}\right) \quad (1\text{-}13)$$

The half-power beamwidth Θ_h can be found once the angles of the first maximum (θ_m) and the half-power point (θ_h) are found. For a symmetrical pattern

$$\Theta_h = 2|\theta_m - \theta_h| \quad (1\text{-}14)$$

1.2.2 Broadside Array

In many applications it is desirable to have the maximum radiation of an array directed normal to the axis of the array (broadside; θ =90° of Figure 2.2(a)). To optimize the design, the maxima of the single element and of the array factor should both be directed toward θ = 90°. The requirements of the single elements can be accomplished by the judicious choice of the radiators and those of the array factor by the proper separation and excitation of the individual radiators. In this section, the requirements that allow the array factor to "radiate" efficiently broadside will be developed. Referring to (1-l0c) or (1-10d), the maximum of the array factor

$$\psi = kd\cos\theta + \beta = 0 \qquad (1\text{-}15)$$

Since it is desired to have the maximum directed toward $\theta = 90^0$, then

$$\psi = kd\cos\theta + \beta\Big|_{\theta=90^0} \Rightarrow \beta = o \qquad (1\text{-}15a)$$

Thus to have the maximum of the array factor of a uniform linear array directed broadside to the axis of the array, it is necessary that all the elements have the same phase excitation (in addition to the same amplitude excitation).To ensure that there are no principal maxima in other directions, which are referred to as *grating lobes,* the separation between the elements should not be equal to multiples of a wavelength ,

$(d \neq n\lambda, n = 1,2,3\ldots)$

Where $\beta = 0$.

If $d = n\lambda, n = 1,2,3,....$ Then,

$$\psi = kd\cos\theta + \beta\Big|_{\substack{d=n\lambda \\ \beta=0 \\ n=1,2,3,\ldots}} = 2\pi n\cos\theta\Big|_{\theta=0^0,180^0} = \pm 2n\pi \qquad (1\text{-}16)$$

This value of ψ when substituted in (1-l0c) makes the array factor attain its maximum value. Thus for a uniform array with $\beta = 0, d = n\lambda,$ in addition to having the maxima of the array factor directed broadside *(*θ = 90°) to the axis of the array, there are additional maxima directed along the axis *(*θ = 0°, 180°) of the array (end-fire radiation).

One of the objectives in many designs is to avoid multiple maxima, in addition to the main maximum, which are referred to as *grating lobes.* Often it may be required to select the largest spacing between the elements but with no grating lobes. To avoid any grating lobe the largest spacing-between the elements should be less than one wavelength $(d_{\max} < \lambda)$.

To illustrate the broadside method the three dimensional array factor of a 10-element (N=10) uniform array with $\beta = 0$ and $\mathrm{d} = \lambda/4$ is shown plotted in figure 2.3(a). A 90 degree angular sector has been removed for better view of the pattern distribution in elevation plane. The only maximum occurs at broadside ($\theta = 90^0$). To form a comparison, the three dimensional pattern of the same array for $\mathrm{d} = \lambda$ is also plotted in figure2.3(b). For this pattern, in addition to the maximum at $\theta = 90^0$, there are additional maxima directed toward $\theta = 0^0, 180^0$. The corresponding two-dimensional patterns of figures 2.3(a,b) are shown in figures 2.4(a,b),so when the displacement between the elements is increased ,the side lobe level becomes higher and the number of sidelobes increases. The half-power beamwidth becomes bigger for decreasing displacements between elements. When the displacement is increased up to one wavelength the power is shifted from the mainbeam to the sidelobes (i.e. the sidelobes become the mainbeam).

If the spacing between the elements is chosen between $\lambda < \mathrm{d} < 2\lambda$,then the maximum of figure 2.3 toward $\theta = 0^0$ shifts toward the angular region $0^0 < \theta < 90^0$ while the maximum toward $\theta = 180^0$ shifts toward $90^0 < \theta < 180^0$. When $\mathrm{d} = 2\lambda$, there are maxima toward $0^0, 60^0, 90^0, 120^0$, and 180^0.

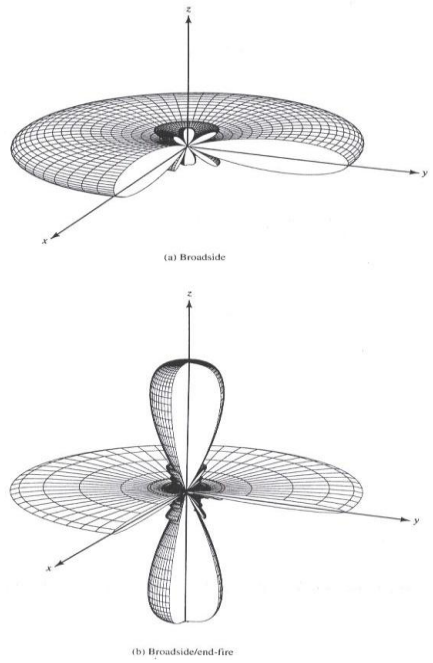

Figure 2.3, Three-dimensional amplitude pattern for (a)broadside, and (b)broadside/end fire arrays.

The expressions for first null beamwidth , half-power beamwidth and first side lobe beamwidth are given by [3] ; the first null Beamwidth (FNBW) is,

$$\Theta_n = 2\left[\frac{\pi}{2} - \cos^{-1}\left(\frac{\lambda}{Nd}\right)\right] \qquad (3\text{-}17)$$

For $\pi d / \lambda \prec 1$, the Half-Power Beamwidth (HPBW) is,

$$\Theta_H = 2\left[\frac{\pi}{2} - \cos^{-1}\left(\frac{1.391\lambda}{\pi nd}\right)\right] \qquad (1\text{-}18)$$

For $\pi d / \lambda \prec 1$, the first Side lobe Beamwidth (FSLBW) is,

$$\Theta_s \approx 2\left[\frac{\pi}{2} - \cos^{-1}\left(\frac{1.391\lambda}{\pi Nd}\right)\right] \qquad (1\text{-}19)$$

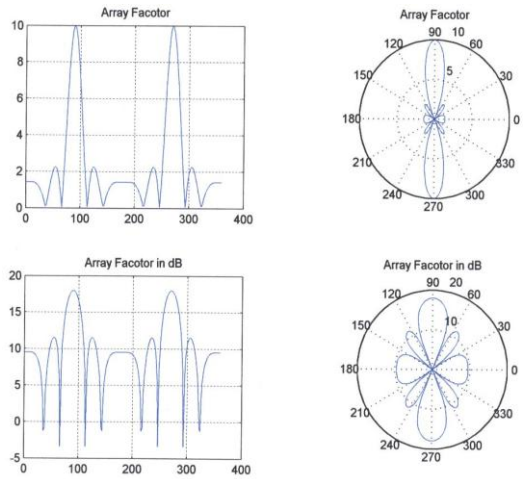

Figure 2.4a, Array factor pattern of a 10-element uniform amplitude broadside array (N=10, $d = \lambda/4, \beta = 0$)

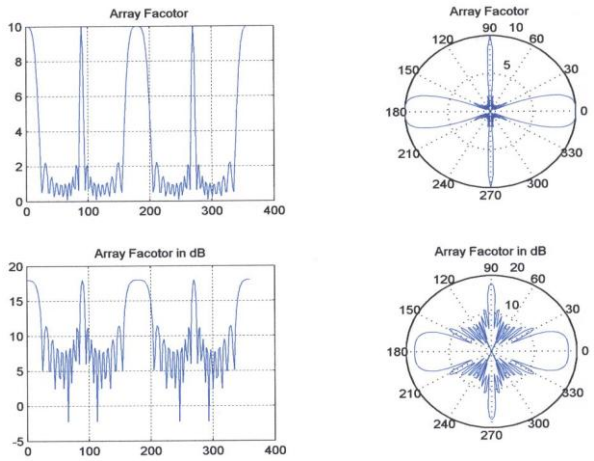

Figure 2.4b, Array factor pattern of a 10-element uniform amplitude broadside array (N=10, $d = \lambda, \beta = 0$)

1.2.3 Ordinary End-Fire Array

Instead of having the maximum radiation broadside to the axis of the array, it may be desirable to direct it along the axis of the array (end-fire). As a matter of fact, it may be necessary that it radiates towards only one direction (either θ = *0*° or 180°).

To direct the maximum toward $\theta = 0^0$

$$\psi = kd\cos\theta + \beta\big|_{\theta=0^0} = kd + \beta = 0 \Rightarrow \beta = -kd \quad \text{(1-20a)}$$

If the maximum is desiredtoward $\theta = 180^0$

$$\psi = kd\cos\theta + \beta\big|_{\theta=180^0} = -kd + \beta = 0 \Rightarrow \beta = kd \quad \text{(1-20b)}$$

Thus end –fire radiation is accomplished when $\beta = -kd(\,for\,\theta = 0^0) or \beta = kd(\,for\,\theta = 180^0)$

If the element separation is d = $\lambda/2$, then the fire radiation exists in both directions at $(\theta = 0^o \, and \, \theta = 180^o).$

If the element spacing is a multiple of a wavelength $(d = n\lambda)$, (n=1,2,3,…), then in addition to having end-fire radiation in both directions there also exist maxima in the broadside directions. Thus for d= $n\lambda$, n =1, 2, 3… There exist four maxima; two in the broadside directions and two along the axis of the array. To have only one end-fire maximum and to avoid any grating lobes, the maximum spacing between the elements should be less than $d_{\max} < \lambda/2.$

The two dimensional patterns of a 10-element (N=10) array with $d = \lambda/4, \beta = +kd$ are plotted in figure 2.5(a). When $\beta = -kd$, the maximum is directed along $\theta = 0^0$ and it is shown in figure 2.5(b). However, when $\beta = +kd$, the maximum is oriented toward $\theta = 180^0$.The characteristics of the array factor can be controlled by choosing the angles 0^0 or 180^0.

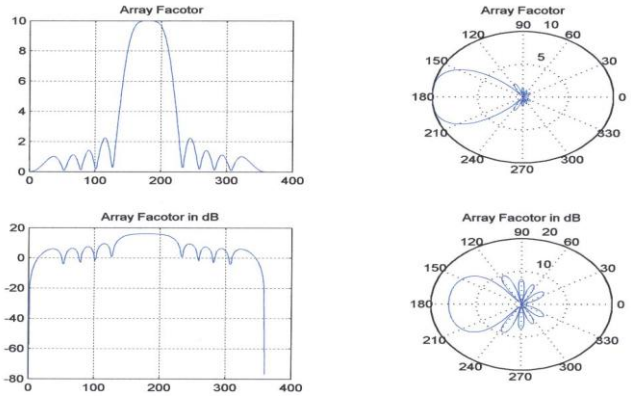

Figure 2.5a, Array factor pattern of a 10-element uniform amplitude end-fire array (N=10, $\mathrm{d} = \lambda/4, \beta = kd$).

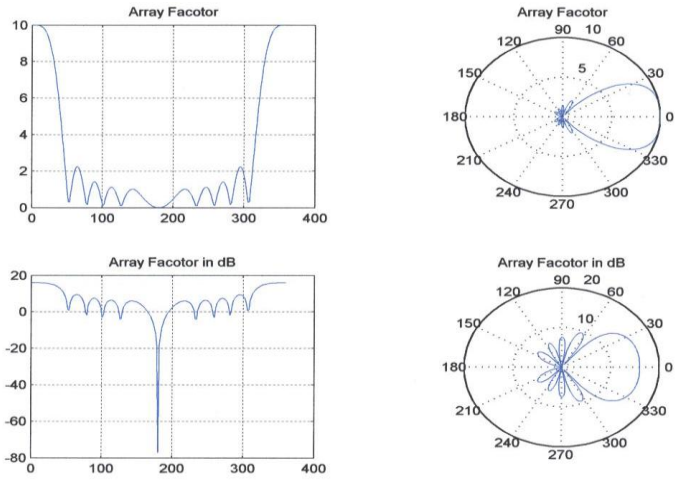

Figure 2.5b, Array factor pattern of a 10-element uniform amplitude end-fire array (N=10, $\mathrm{d} = \lambda/4, \beta = -kd$)

The expressions for first null beamwidth , half-power beamwidth and first side lobe beamwidth are given by [3], First null Beamwidth (FNBW)

$$\Theta_n = 2\cos^{-1}\left(1 - \frac{\lambda}{Nd}\right) \qquad (1\text{-}21)$$

For $\pi d/\lambda \prec 1$, the Half-Power Beamwidth (HPBW) is,

$$\Theta_H = 2\cos^{-1}\left(1 - \frac{1.391\lambda}{\pi Nd}\right) \qquad (1\text{-}22)$$

For $\pi d/\lambda \prec 1$, the first Side lobe Beamwidth (FSLBW) is,

$$\Theta_s \approx 2\cos^{-1}\left(1 - \frac{3\lambda}{\pi Nd}\right) \qquad (1\text{-}23)$$

1.2.4 Phased (Scanning) Array

In the previous two sections it was shown how to direct the major radiation from an array, by controlling the phase excitation between the elements, in directions normal (broadside) and along the axis (end-fire) of the array. It is then logical to assume that the maximum radiation can be oriented in any direction to form a scanning array. The procedure is similar to that of the previous two sections.

Let us assume that the maximum radiation of the array is required to be oriented at an angle $\theta_0 \, (0^o \le \theta_0 \le 180^o)$. To accomplish this, the phase excitation β between the elements must be adjusted so that,

$$\psi = kd\cos\theta + \beta\big|_{\theta=\theta_0} = kd\cos\theta_0 + \beta = 0 \Rightarrow \beta = -kd\cos\theta_0 \quad (1\text{-}24)$$

Thus by controlling the progressive phase difference between the elements, the maximum radiation can be squinted in any desired direction to form a scanning array. This is the basic principle of electronic scanning phased array operation. Since in phased array technology the scanning must be continuous, the system should be capable of continuously varying the progressive phase between the elements. In practice, this is accomplished electronically by the use of ferrite or diode phase shifters. For ferrite phase shifters, the phase shift is controlled by the magnetic field within the ferrite, which in turn is controlled by the amount of current flowing through the wires wrapped around the phase shifter.

For diode phase shifter using balanced, hybrid-coupled varactors, the actual phase shift is controlled either by varying the analog bias dc voltage (typically 0-30 volts) or by a digital command through a digital-to-analog (D/A) converter [8].

To demonstrate the principle of scanning , the two-dimensional pattern of a 10-element array, with a separation of $\lambda/4$ between the elements and with the maximum squinted in the $\theta_0 = 60^0$ direction, is plotted in Figure 2.6. So the characteristics of the array factor can be controlled by choosing the scanning angle

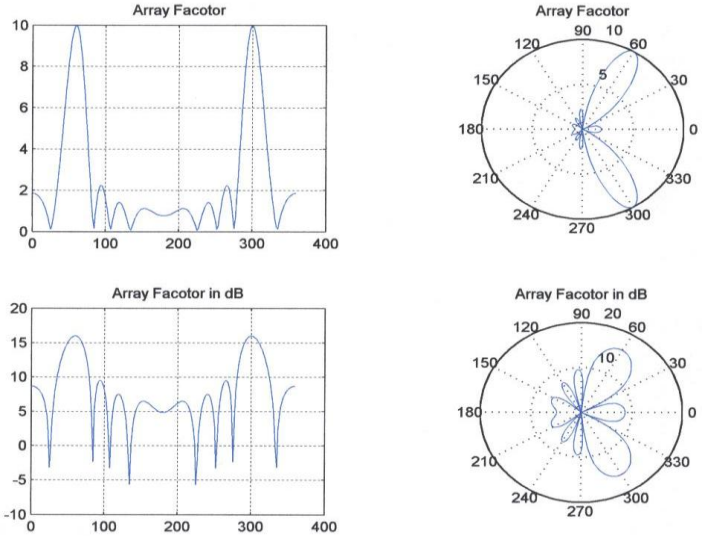

Figure 2.6, Array factor pattern of a 10-element uniform amplitude scanning array (N=10, $d = \lambda/4, \beta = -kd*\cos(\theta_0), \theta_0 = 60^0$).

The half-power beamwidth of the scanning array is obtained with $\beta = -kd\cos\theta_0$. Using the minus sign in the argument of the inverse cosine function in (1-14) to represent one angle of the half-power beamwidth and the plus sign to represent the other angle, then the total beanwidth is the difference between these two angles and can be written as [3],

Since N= (L+d)/d,

$$\Theta_s = \cos^{-1}\left[\cos\theta_0 - 0.443\frac{\lambda}{(L+d)}\right] - \cos^{-1}\left[\cos\theta_0 + 0.443\frac{\lambda}{(L+d)}\right] \quad (1\text{-}25)$$

where L is the length of the array.

1.2 The Analysis Of A Spherical Phased Array Antenna

The Spherical Phased Array (SPA) is a true 3-D array designed to operate in the microwave region. The analytical approach presents a simplified model for this mathematically complex problem. The results are encouraging and show the unique steering capability of this array to scan beyond the horizon without serious tradeoffs in beam width or side lobes characteristics.

The purpose of designing a spherically arrayed antenna is to be able to maximize beam steering. In practice, however, the beam steering will have to exclude the feed region of the array. The Spherical Phased Array (SPA) antenna is composed of identical antennas distributed over the surface of a sphere. As a first level of analysis, the antennas assumed to be isotropic with well defined distribution. To simplify the analysis, a structural approach is utilized. This implies the development of the full SPA analysis by adding the contributions of partial set structures to form the final spherical geometry. A circular array will be considered first. The far field expression for the SPA is then obtained by the application of pattern multiplication techniques.

The basic analysis for an antenna array system starts with the proper definition of the coordinate system followed by the calculation of the phase shift presented by each element in the array. The analysis of the SPA antenna system follows the same logic.

Given a spherical coordinate system and letting R be the position of an isotropic point source from the origin and r defines the position of the far field point where it is being measured, then the phase shift ψ_i measured at that point is given by [4],

$$\psi_i = kRCos\delta_i + \alpha_i \qquad (1\text{-}26)$$

Where k is the phase constant $2\pi/\lambda$, α_i is the phase shift associated with the excitation of the *ith* source, and δ_i is defined b y the equation,

$$Cos\delta_i = Sin\theta_i \cos\phi_i Sin\theta Cos\phi + Sin\theta_i Sin\phi_i Sin\theta Sin\phi + Cos\theta_i Cos\theta \qquad (1.27)$$

1.2.1 The Far Field of Circular array

First consider a system of four point sources arranged in a circular array in the XY plane as shown in Figure 2.7

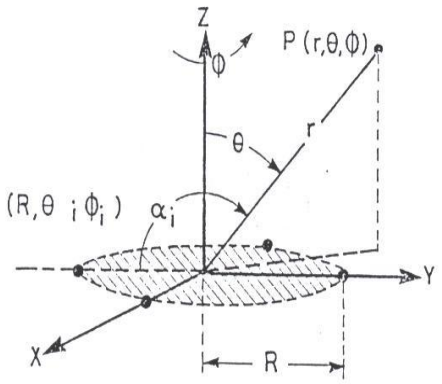

Figure 2.7, four point source circular Array

Furthermore, assume that the source excitations phase shifts are zero $(\alpha_i = O)$ and taking into account that the sign of the phase shift need not be considered since it will be determined by the sign of the cosine function. In the case of a circular array, with an even number of point sources, each point source will have an opposite point source about the origin with an equal in magnitude but opposite in sign.

The respective phase shifts for each of the four point sources can be calculated using Equations (1.26) and (1-27) as given below,

$$\psi_1 = kR[Sin\theta Cos\phi] = -\psi_3 \qquad (1\text{-}28)$$

$$\psi_2 = kR[Sin\theta Sin\phi] = -\psi_4 \qquad (1.29)$$

And the electric field in the r direction for the array will then be defined by,

$$E_r = E_0[e^{i\psi_1} + e^{i\psi_2} + e^{i\psi_3} + e^{i\psi_4}]$$
$$= E_0[2Cos(kRSin\theta Cos\phi) + 2Cos(kRSin\theta Sin\phi)]$$
(1.30)

And the array factor is deified by,

$$A_F = E_r / E_0$$

$$A_F = 2[Cos(kRSin\theta Cos\phi) + Cos(kRSin\theta Sin\phi)] \quad (1.31)$$

Where E_0 is the magnitude of the electric field at the source. As expected this array factor yields a zero phase shift because the far field pattern was taken with respect to the center of the circular array.

Continuing the build up of the SPA, consider now the case with two circular array systems. This new combination has the phase reference located at the origin of the coordinate system so that the phase angle of the far field pattern of the system will also be zero. If these two circular arrays are considered to be lying on the surface of a sphere of radius R, whose center is the center of the coordinate system, then a new parameter will be needed to define the circular array's position on the sphere. This parameter will be designated by θ_i. As can be seen, from Figure 2.8 below; this angle will define the position of both arrays on the surface of the sphere. The distance of the circular array from the origin and its radius is defined by $(RCos\theta_i)$ and $(RSin\theta_i)$, respectively.

The array factor for each of the circular arrays can be determined from equation (1.31). Hence,

$$A_{Fci} = 2[Cos(kRSin\theta Cos\phi \sin\theta_i) + Cos(kRSin\theta Sin\phi \sin\theta_i)]$$
(1.32)

Now let the phase center (center of the circle on which the point source lie) of each of these two circular arrays is considered to be a point source. Consequently, the array factor defining these two point sources is given by,

$$A_{Fsi} = 2Cos(kRCos\theta_i Cos\theta) \quad (1.33)$$

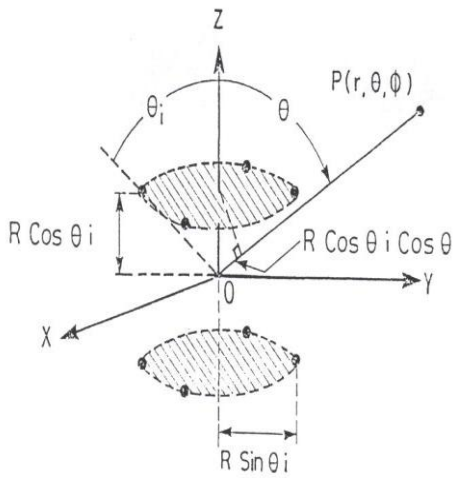

Figure 2.8, Two Circular Array Configurations

The far field pattern for the eight point source array of Figure 2.8 can now be calculated using pattern multiplication. Multiplying Equations (1.32) and (1.33) yields,

$$A_{FT} = A_{Fci} * A_{Fsi}$$
$$= 4Cos(kRCos\theta_i Cos\theta)[Cos(kRSin\theta Cos\phi Sin\theta_i) + Cos(kRSin\theta Sin\phi Sin\theta_i)]$$
(1.34)

The importance of Equation (1.34) is that a method has been devised to determine the radial far field for circular arrays that lie anywhere on a sphere

For eight source array at the center, the array factor for uniform circular array of 8 elements at center can be written as [4],

$$AF(\theta,\phi) = 2\cos(kR\sin(\theta)\cos(\phi)) + 2\cos(kR\sin(\theta)\sin(\phi))$$

$$+ 4\cos(kR\sin(\theta)\frac{\cos(\phi)}{\sqrt{2}})\cos(kR\sin(\theta)\frac{\sin(\phi)}{\sqrt{2}}) \quad (1.35)$$

Figure 2.9 shows the three dimensional pattern of the array factor for a 8-element uniform circular array of radius R= λ. The figure shows that the main lobe to side lobe ratio is 2.7257.

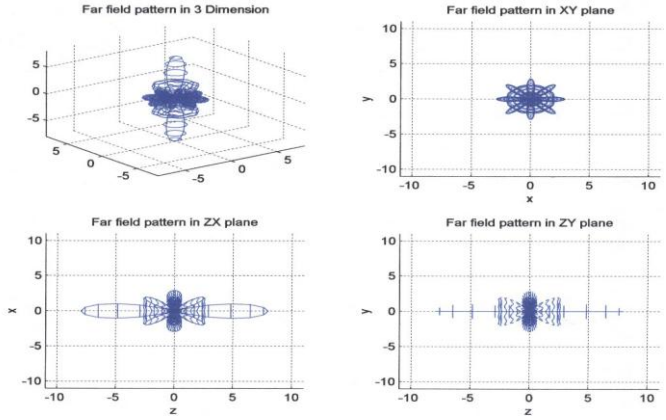

Figure 2.9, Three-dimensional amplitude pattern of the array factor for a uniform circular array of 8-elements of radius R= λ.

1.2.3 The Spherical Phased Array Antenna

The circular arrays studied before can be brought together to form a three dimensional SPA as shown in Figure 2.10. The outline can be visualized as a combination of five symmetric circular arrays. Two one-source arrays at the top and bottom, two four –source arrays, and one eight-source array at the center. This configuration is used for illustration purposes. Many others may be constructed with a varying number of sources and arrangements.

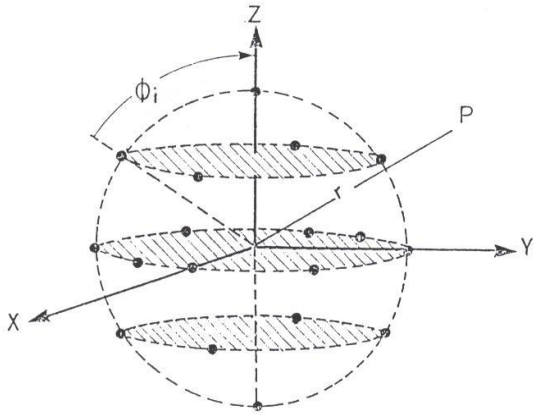

Figure 2.10, Spherical Phased Array Configuration

The equation describing the far field pattern for the SPA Shown in Figure 2.10 is given by the following equation [4],

$$A_{Fspa} = 2\cos(kRCos\theta) + 2Cos(kR\sin\theta Cos\phi) + 2Cos(kRSin\theta Sin\phi)$$
$$+ 4\cos(kR\sin\theta\frac{\cos\phi}{\sqrt{2}})\cos(kR\sin\theta\frac{\sin\phi}{\sqrt{2}})$$
$$+ 4Cos(kRCos\theta_i Cos\theta)[Cos(kRSin\theta_i Sin\theta Cos\phi + Cos(kRSin\theta_i Sin\theta Sin\phi)] \quad (1.36)$$

Figure 2.11 represents a computer generated far field pattern for an SPA antenna configured as shown in figure 2.10 by setting $R = \lambda, and\theta_i = 30^o$.The figure shows the main lobe to side lobe ratio ; it is 3.1062. So it is bigger from the ratio in figure 2.9 which is for an 8-element uniform circular array of radius R= λ. The figure 2.12 shows the two-dimensional pattern of SPA of figure 2.11 for equal amplitude and phase

excitation, ($\phi = 0^0$ (x-z plane) $\phi = 90^0$ (y-z plane)).

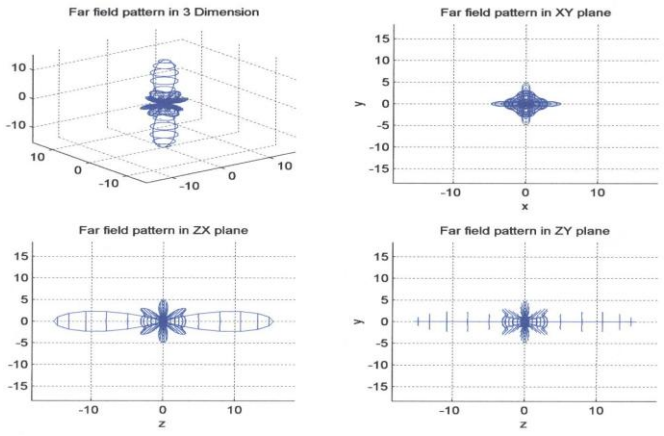

Figure 2.11, Three-dimensional antenna pattern of SPA with $R = \lambda, \theta_i = 30^0, \beta = 0$,and equal amplitude and phase excitation.

1.2.4 The Beam Steering in Spherical Phased Array Antenna

The maximum points can be established in any direction by applying the proper α_i to each point source. The specific values for each of the α_i can be calculated by using Equations (1.26) and letting $\psi_i = 0.$ That is to say,

$$\psi_i = kRCos\delta_i + \alpha_i = 0 \qquad (1.37)$$

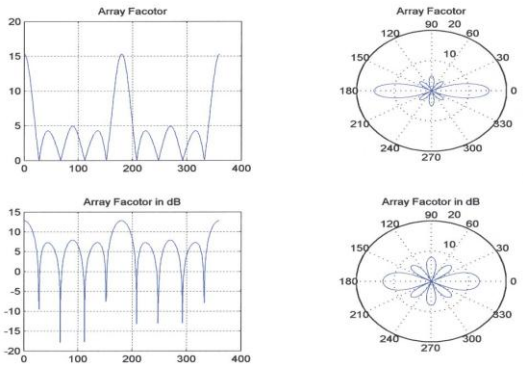

Figure 2.12, Two-dimensional pattern of SPA with $R = \lambda, \theta_i = 30^0, \beta = 0$, and equal amplitude and phase excitation. ($\phi = 0^0$ (x-z plane) $\phi = 90^0$ (y-z plane))

If the required direction in which the electric field is to have its maximum value $\theta = \theta_s, and \phi = \phi_s,$ then the total phase shift of each source should be zero in that direction.

Applying Equation (1.37) to each source and using Figure (2.7), the required excitation phase shifts will then be,

$$\alpha_1 = -kR(Sin\theta_s Cos\phi_s) = -\alpha_3 \qquad (1.38)$$

$$\alpha_2 = -kR(Sin\theta_s Sin\phi_s) = -\alpha_4 \qquad (1.39)$$

Notice that the excitation phase shifts, α_i are constants dependent on the directions in which the beam is to be steered. The total phase shifts for each point source in terms of steer angles is given by,

$$\psi_1 = kR[Sin\theta Cos\phi - Sin\theta_s Cos\phi_s] = -\psi_3 \quad (1.40)$$

$$\psi_2 = kR[Sin\theta Sin\phi - Sin\theta_s Sin\phi_s] = -\psi_4 \quad (1.41)$$

And the corresponding far field expression for the circular array follows to be,

$$A_F = 2[CoskR(Sin\theta Cos\phi - Sin\theta_s Cos\phi_s) + CoskR(Sin\theta Sin\phi - Sin\theta_s Sin\phi_s)] \quad (1.42)$$

Comparing Equation (1.31) and (1.42), the term $(Sin\theta Cos\phi)$ is replaced with $(Sin\theta Cos\phi - Sin\theta_s Cos\phi_s)$ and $(Sin\theta Sin\phi)$ is replaced with $(Sin\theta Sin\phi - Sin\theta_s Sin\phi_s)$.

Consequently, the equation describing the far field pattern of the SPA antenna shown in Figure 5.4 can now be calculated in terms of the steer angles. This equation is given as follows [4] :

$$\begin{aligned} A_{Fspa} &= 2\cos[kR(Cos\theta - Cos\theta_s)] + 2Cos[kR(Sin\theta Cos\phi - Sin\theta_s Cos\phi_s)] \\ &+ 2Cos[kR(Sin\theta Sin\phi - Sin\theta_s Sin\phi_s)] \\ &+ 4\{Cos[kR(Sin\theta Cos\phi - Sin\theta_s Cos\phi_s)/\sqrt{2}]\}\{Cos[kR(Sin\theta Sin\phi - Sin\theta_s Sin\phi_s)/\sqrt{2}]\} \\ &+ 4Cos[kRCos\theta_i(Cos\theta - Cos\theta_s)]\{Cos[kRSin\theta_i(Sin\theta Cos\phi - Sin\theta_s Cos\phi_s)] \\ &+ Cos[kRSin\theta_i(Sin\theta Sin\phi - Sin\theta_s Sin\phi_s)]\} \end{aligned} \quad (1.43)$$

Again, one should note the similarity between Equation (1.43) and Equation (1.36), which describes the far field pattern without any phase shift applied to the excitation.

The following figures represent the far field pattern for the SPA antenna described in Figure 1.30 with R = 0.75 λ and $\theta_i = 30^o$. These are picked for demonstration purposes and other combinations are possible to steer the beam in the desired direction. The steer angles θ_s and ϕ_s were varied to exhibit the steering capability of the array. Figures 2.13 and 2.14 demonstrate these phenomena where the main lobe was moved from $\phi = 0^o to \phi = 90^o$ keeping θ constant at 90^0 (horizontal plane). Figures 2.15 and 2.16 show the ability to steer the array from $\theta = 0^o to \theta = 180^o$ (vertical plane), respectively. Figure 2.17 shows two dimensional pattern of the SPA with equal amplitude and a scanning angle $\theta_S = 60^0$, ($\phi = 0^0$ (x-z plane) $\phi = 90^0$ (y-z plane)) . Figures 2.18, 2.19 and 2.20 show three dimensional pattern of the SPA with equal amplitude and scanning angle $\theta_S = 60^0, \phi_S = 0^0, 90^0, 45^0$ respectively. So the characteristic of the array factor can be controlled in 3-dimension by changing the phase shifts for each point source in terms of steer angles.

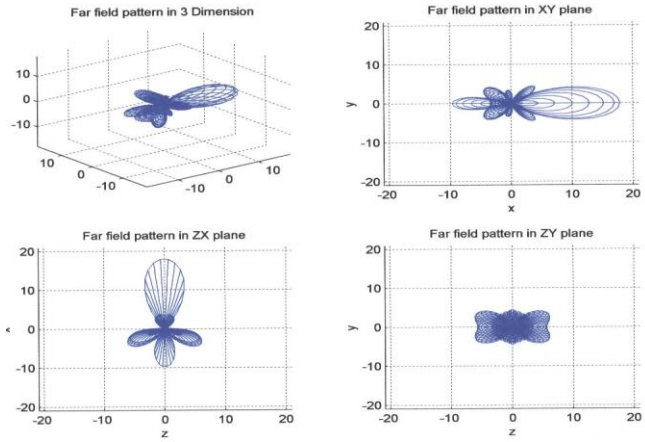

Figure 2.13, Three dimensional pattern of a SPA with a $R = .75\lambda, \theta_i = 30^0$, and equal amplitude and scanning angle $\theta_S = 90^0, \phi_S = 0^0$.

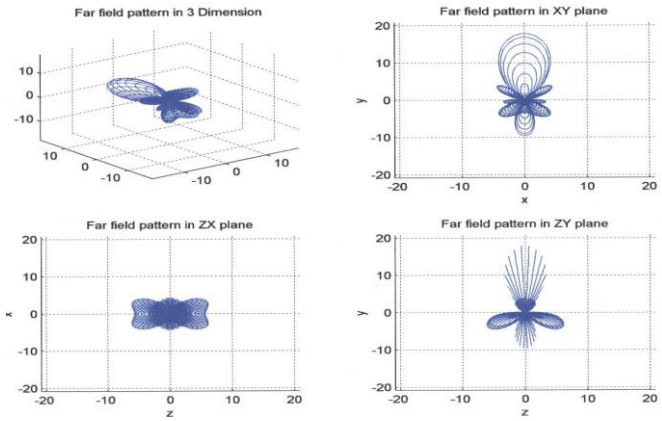

Figure 2.14, Three dimensional pattern of a SPA with a $R = .75\lambda, \theta_i = 30^0$, and equal amplitude and scanning angle $\theta_S = 90^0, \phi_S = 90^0$.

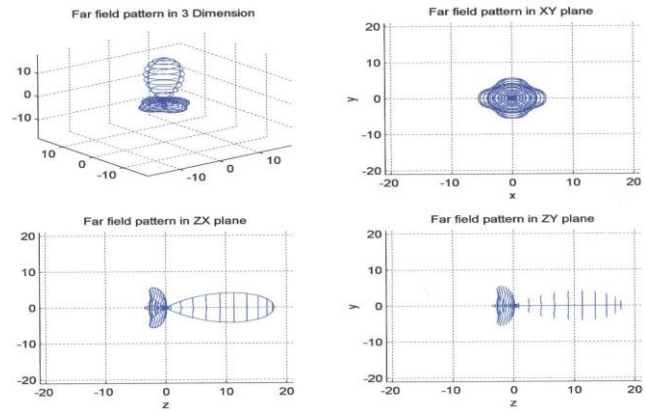

Figure 2.15, Three dimensional pattern of a SPA with a $R = .75\lambda, \theta_i = 30^0$, and equal amplitude and scanning angle $\theta_S = 0^0, arbitray\_\phi_S$.

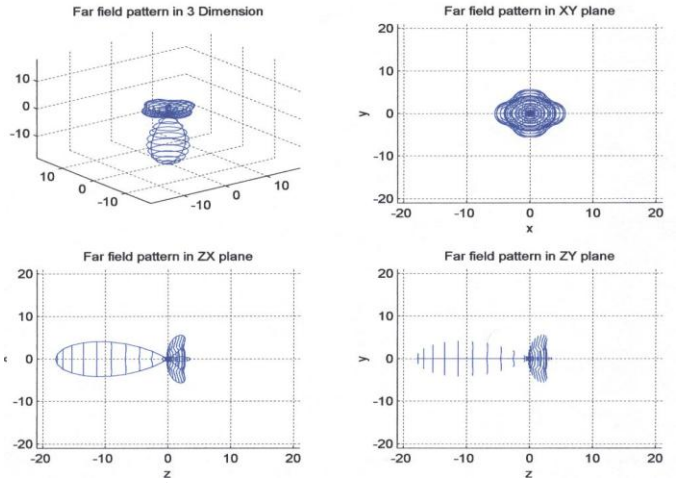

Figure 2.16, Three dimensional pattern of a SPA with a $R = .75\lambda, \theta_i = 30^0$, and equal amplitude and scanning angle $\theta_S = 180^0, arbitray\_\phi_S$.

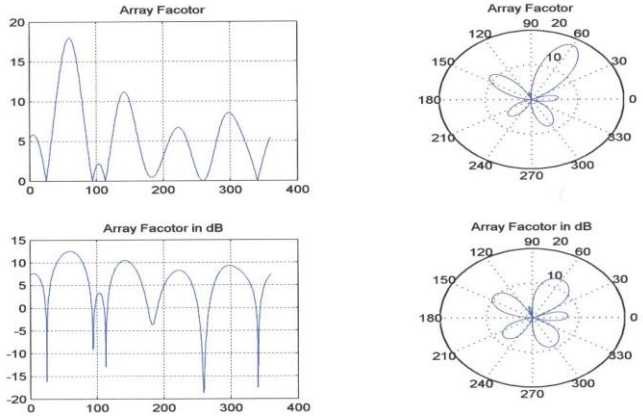

Figure 2.17, Tow dimensional pattern of a SPA with a $R = .75\lambda, \theta_i = 30^0$, and equal amplitude and scanning angle. $\theta_S = 60^0$. ($\phi = 0^0$ (x-z plane)).

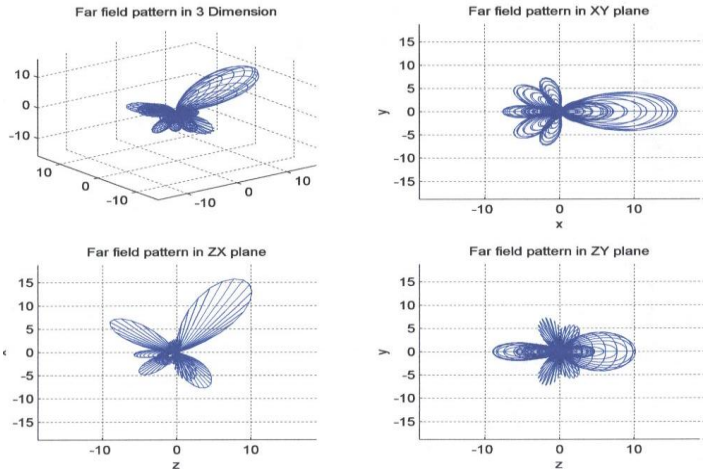

Figure 2.18, Three dimensional pattern of a SPA with a $R = .75\lambda, \theta_i = 30^0$, and equal amplitude and scanning angle $\theta_S = 60^0, \phi_S = 0^0$.

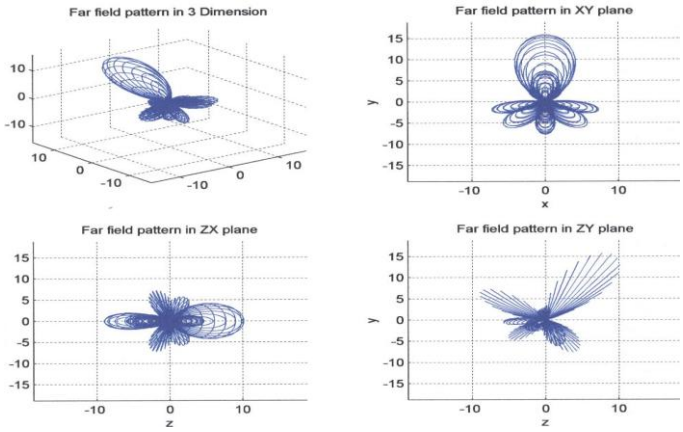

Figure 2.19, Three dimensional pattern of a SPA with a $R = .75\lambda, \theta_i = 30^0$, and equal amplitude and scanning angle $\theta_S = 60^0, \phi_S = 90^0$.

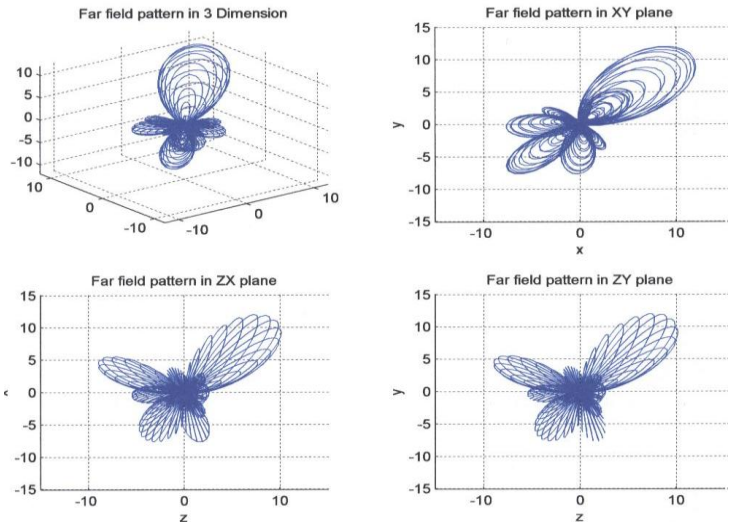

Figure 2.20, Three dimensional pattern of a SPA with $R = .75\lambda, \theta_i = 30^0$, and equal amplitude and scanning angle $\theta_S = 60^0, \phi_S = 45^0$.

2 Optimazation For Spherical Phased Array Antenna

2.1 Derivation Of General Equation For SPA Antenna

The spherical phased Array antenna is composed of identical feeding sources distributed over the surface of a sphere. Proposed spherical array model is adopted using the Array Factor equation $AF(\theta, \phi)$ of general spherical phased array antennas.

The SPA can be segmented into many sections with each one as a circular array. Given a spherical coordinate system and letting "a" be the position of an isotropic point source w.r.t. the origin and "r" defines the position of the far field point where it is being measured, then the progressive phase ψ_n measured at that point is given by [4] :

$$\psi_n = ka\cos(\delta_n) + \alpha_n \qquad (1.44)$$

Where k is the phase constant $(\frac{2\pi}{\lambda})$.

a: is the radius of circular array at the central circle.

α_n : is the progressive phase shift associated with excitation of the n_th source.

δ_n : is defined by the equation:

$$Cos\delta_n = Sin\theta_m \cos\phi_n Sin\theta Cos\phi + Sin\theta_m Sin\phi_n Sin\theta Sin\phi + Cos\theta_m Cos\theta$$

(145a)

And defined in general by the equation:

$$\cos(\delta_n) = \sin(\theta_m)\sin(\theta).\cos(\phi - \phi_n) + \cos(\theta_m)\cos(\theta)$$

(1.45b)

Where

N= Number of elements in each circular section.

M= Number of circular sections of the sphere.

n is the n_th element source in circular array.

m is the m_th section in the whole spherical array.

θ_m = angle of the position of circular array on the surface of the sphere.

ϕ_{nm} = angular position of n_th element on m_th section.

$$\phi_{nm} = 2\pi(\frac{n}{N}) \qquad (1.46)$$

I_{nm} = amplitude excitation of the n_th element on m_th section.

The Array factor of (SPA) can be written in the following form :

$$AF(\theta,\phi) = \sum_{m=1}^{M}\sum_{n=1}^{N} I_{nm} e^{i[ka(\sin(\theta_m)\sin(\theta)\cos(\phi-\phi_n)+\cos(\theta_m)\cos(\theta))+\alpha_n]}$$

(1.47)

where

$$\alpha_n = -ka\left[Sin\theta_m Sin\theta(Cos(\phi - \phi_n)) + \cos\theta_m \cos\theta\right]$$

(1.48)

The maximum points can be established in any direction by applying the proper α_i to each point source. The specific values for each of the α_i can be calculated by using equation (1.44) and letting $\psi_i = 0.$ If the required direction in which the electric field is to have its maximum value $\theta = \theta_s, and \phi = \phi_s,$ then the total phase shift of each source should be zero in that direction.

Case studies :

The following case studies I, II and III will prove the general formula of the spherical phased array antenna.

Case study I

As shown in figure 6.1 , four point source Circular Array at center of the sphere where,

$M = 1$ at $\theta_m = \frac{\pi}{2}$ and $\alpha_n = 0$

The array factor is given by,

$$AF(\theta,\phi) = \sum_{n=1}^{N} I_n . e^{i[ka(\sin(\theta)\cos(\phi-\phi_n))+\alpha_n]}$$

From the figure we have N= 4 and $\phi_n = 0, \pi/2, \pi, 3\pi/2$, respectively,

and let $I_n = 1$ and $\alpha_n = 0$

$$AF(\theta,\phi) = e^{i\psi_1} + e^{i\psi_2} + e^{i\psi_3} + e^{i\psi_4}$$

where

$$\psi 1 = ka.\sin(\theta).\cos(\phi - 0) = ka\ .\sin(\theta).\cos(\phi)$$
$$\psi 2 = ka.\sin(\theta).\cos\left(\phi - \frac{\pi}{2}\right) = ka\ .\sin(\theta).\sin(\phi)$$
$$\psi 3 = ka.\sin(\theta).\cos(\phi - \pi) = -ka\ .\sin(\theta).\cos(\phi)$$
$$\psi 4 = ka.\sin(\theta).\cos\left(\phi - \frac{3\pi}{2}\right) = -ka\ .\sin(\theta).\sin(\phi)$$

$$AF(\theta,\phi) = 2\cos(ka\ \sin(\theta)\cos(\phi)) + 2\cos(ka\sin(\theta)\sin(\phi))$$

So it is the same as the equation (1.31)

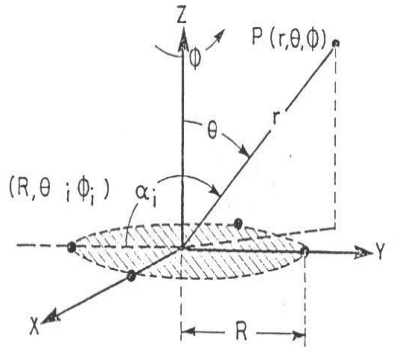

Figure 2.19, Four point source Circular Array

Case study II

For figure 2.20, two Circular Array Configurations are considered where,

$$M = 2 \qquad \text{at } \theta_m = \theta_1 \qquad \alpha_n = 0$$

$$AF(\theta,\phi) = \sum_{m=1}^{2}\ \sum_{n=1}^{4} I_n.e^{i[ka((\sin(\theta)\sin(\theta_1)\cos(\phi-\phi_n)+\cos(\theta_1)\cos(\theta)+\alpha_n]}$$

We have N= 4 and $\phi_n = 0, \pi/2, \pi, 3\pi/2$, respectively, and let $I_n = 1$ and $\alpha_n = 0$ for the tow circular array configurations. For the upper circular array,

$$AF_1(\theta,\phi) = \left(e^{i\psi_1} + e^{i\psi_2} + e^{i\psi_3} + e^{i\psi_4}\right)$$

Where,

$$\psi_1 = ka\left[(\sin(\theta_1).\sin(\theta)\cos(\phi)) + \cos(\theta_1)\cos(\theta)\right]$$
$$\psi_2 = ka\left[(\sin(\theta_1).\sin(\theta)\sin(\phi)) + \cos(\theta_1)\cos(\theta)\right]$$
$$\psi_3 = ka\left[-(\sin(\theta_1).\sin(\theta)\cos(\phi)) + \cos(\theta_1)\cos(\theta)\right]$$
$$\psi_4 = ka\left[-(\sin(\theta_1).\sin(\theta)\sin(\phi)) + \cos(\theta_1)\cos(\theta)\right]$$

$$AF_1(\theta,\phi) = 2e^{ika.\cos(\theta_1)\cos(\theta)}.(\cos(ka.\sin(\theta)\sin(\theta_1).\cos(\phi)) + \cos(ka.\sin(\theta_1)\sin(\theta).\sin(\phi)))$$

Applying the same method for the dawn section, we have

$$AF_2(\theta,\phi) = 2e^{-ika.\cos(\theta_1)\cos(\theta)}.(\cos(ka.\sin(\theta)\sin(\theta_1).\cos(\phi)) + \cos(ka.\sin(\theta_1)\sin(\theta).\sin(\phi)))$$

Then,

$$AF_{total}(\theta,\phi) = AF_1(\theta,\phi) + AF_2(\theta,\phi)$$

$$AF_{total}(\theta,\phi) = 4\cos(ka.\cos(\theta_1)\cos(\theta)).(\cos(ka.\sin(\theta)\sin(\theta_1).\cos(\phi)) + \cos(ka.\sin(\theta_1)\sin(\theta).\sin(\phi)))$$

So it is the same as the equation (1.34)

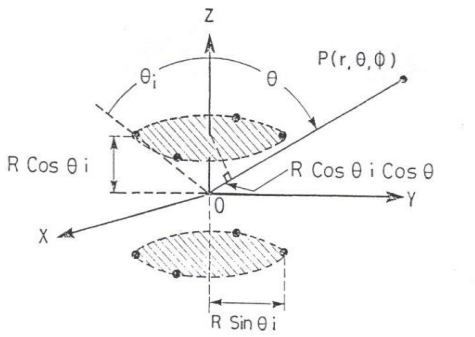

Figure 2.20, Two Circular Array Configurations

Case study III
As shown in figure 2.21, Spherical Phased Array Configuration where,

$M = 5$ at $\theta_m = 0, \theta_1, \pi/2$ $\alpha_n = 0$

i) In the first two sections from the figure, we have $\theta_m = 0$, $I_n = 1$, N=1,

$$AF_1(\theta,\phi) = \sum_{m=1}^{2}\sum_{n=1}^{1} I_n . e^{i[ka((\sin(\theta)\sin(\theta_m)\cos(\phi-\phi_n)+\cos(\theta_m)\cos(\theta)+\alpha_n]}$$

$$AF_1(\theta,\phi) = e^{i[ka\cos(\theta_m)\cos(\theta)]} + e^{-i[ka\cos(\theta_m)\cos(\theta)]}$$

$$AF_1(\theta,\phi) = 2\cos(ka(\cos(\theta)))$$

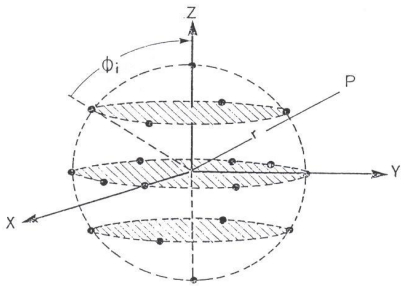

Figure 2.21, Spherical Phased Array Configuration

ii) In the second two sections from the figure, we have
$\phi_n = 0, \pi/2, \pi, 3\pi/2$, respectively and $I_n = 1$, $N = 4$.
Then the array factor is,

$$AF_2(\theta,\phi) = \sum_{m=1}^{2}\sum_{n=1}^{4} I_n . e^{i[ka((\sin(\theta)\sin(\theta_m)\cos(\phi-\phi_n)+\cos(\theta_m)\cos(\theta)+\alpha_n]}$$

$$AF_2(\theta,\phi) = 2\cos(ka.\cos(\theta_1)\cos(\theta)).(2\cos(ka.\sin(\theta_1).\sin(\theta).\cos(\phi)) + 2\cos(ka.\sin(\theta_1)\sin(\theta).\sin(\phi)))$$

iii) The 5_th section at the center of the sphere has eight sources where,

$N = 8, \theta_m = \frac{\pi}{2}$

$\phi_n = 0, \pi/4, \pi/2, 3\pi/4, \pi, 5\pi/4, 3\pi/2, 7\pi/4,$ *respectively* and $I_n = 1$

$$AF_3(\theta,\phi) = \sum_{m=1}^{1}\sum_{n=1}^{8} I_n . e^{i[ka((\sin(\theta)\sin(\theta_m)\cos(\phi-\phi_n)+\cos(\theta_m)\cos(\theta)+\alpha_n]}$$

$$AF_3(\theta,\phi) = \left[\sum_{n=1}^{8} e^{i[ka(\sin(\theta)\cos(\phi-\phi_n)]}\right]$$

$$AF_3(\theta,\phi) = e^{i\psi_1} + e^{i\psi_2} + e^{i\psi_3} + e^{i\psi_4} + e^{i\psi_5} + e^{i\psi_6} + e^{i\psi_7} + e^{i\psi_8}$$

Where

$$\psi_1 = ka\sin(\theta)\cos(\phi)$$

$$\psi_2 = ka\sin(\theta)\cos(\phi - \frac{\pi}{4}) = ka\left(\sin(\theta)\frac{\cos(\phi)}{\sqrt{2}} + \sin(\theta)\frac{\sin(\phi)}{\sqrt{2}}\right)$$

$$\psi_3 = ka\sin(\theta)\cos(\phi - \frac{\pi}{2}) = ka\sin(\theta)\sin(\phi)$$

$$\psi_4 = ka\sin(\theta)\cos(\phi - \frac{3\pi}{4}) = ka\left(-\sin(\theta)\frac{\cos(\phi)}{\sqrt{2}} + \sin(\theta)\frac{\sin(\phi)}{\sqrt{2}}\right)$$

$$\psi_5 = -\psi_1$$

$$\psi_6 = ka\sin(\theta)\cos(\phi - \frac{5\pi}{4}) = ka\left(-\sin(\theta)\frac{\cos(\phi)}{\sqrt{2}} - \sin(\theta)\frac{\sin(\phi)}{\sqrt{2}}\right)$$

$$\psi_7 = -\psi_3$$

$$\psi_8 = ka\sin(\theta)\cos(\phi - \frac{7\pi}{4}) = ka\left(\sin(\theta)\frac{\cos(\phi)}{\sqrt{2}} - \sin(\theta)\frac{\sin(\phi)}{\sqrt{2}}\right)$$

$$AF_3(\theta,\phi) = 2\cos(ka\sin(\theta)\cos(\phi)) + 2\cos(ka\sin(\theta)\sin(\phi))$$
$$+ 4\cos(ka\sin(\theta)\frac{\cos(\phi)}{\sqrt{2}})\cos(ka\sin(\theta)\frac{\sin(\phi)}{\sqrt{2}})$$

Applying superposition principle, the array factor of the spherical array antenna is given by:

$$AF_{total}(\theta,\phi) = AF_1(\theta,\phi) + AF_2(\theta,\phi) + AF_3(\theta,\phi)$$

$$AF_{total}(\theta,\phi) = 2\cos(ka.\cos(\theta_1)\cos(\theta)).(2\cos(ka.\sin(\theta_1).\sin(\theta).\cos(\phi)) + 2\cos(ka.\sin(\theta_1)\sin(\theta).\sin(\phi))$$
$$+ 2\cos(ka(\cos(\theta))) + 2\cos(ka\sin(\theta)\cos(\phi)) + 2\cos(ka\sin(\theta)\sin(\phi))$$
$$+ 4\cos(ka\sin(\theta)\frac{\cos(\phi)}{\sqrt{2}})\cos(ka\sin(\theta)\frac{\sin(\phi)}{\sqrt{2}})$$

It was found that $AF_{total}(\theta,\phi)$ is the same as that in equation (1.36)

The derived equations have been programmed using matlab software, and it was applied to the model of reference [4]. The running results obtained were typically the same as that of equation (1.36) of reference [4].

The general equation (1.47) can be applied to the circular phased array Antenna by substituting for M=1, θ_m =90. The results obtained matched well with equation (4-18a) P.79.

3. General phased Array (GPA) antennas program

The program GPA–2D can draw the array factor in 2- Dimension with respect to linear (uniform and nonuniform amplitude), planner, circular and spherical phased array antennas. However, the program GPA–3D can draw the array factor in 3- Dimension with respect to planar, circular and spherical phased array antennas. Moreover, two main programs are added and extended by Visual Matlab. The GPA program is used to draw the array factor in two and three dimensions.

Using these programs, any phased Array antenna configuration can be analyzed simply by stating its parameters in these general programs.

4. Optimazation For Spherical Phased Array Antenna

4.1 Optimization of 5-sections SPA antenna

By using matlab software program (OPT-M5) optimized results for 5-sections of SPA antenna (Broad side array) have been obtained by scanning for radius, number of elements in each section , and angle of the section w.r.t the center sphere.

The normalized lobe ratio (main lobe intensity to side lobe intensity) becomes smaller if the radius of the sphere is less than one wavelength ($a < \lambda$).

Three main cases have been discussed.

Case I: The best normalized result is obtained when, $a/\lambda = 1$, N = [1 10 10] and $\theta_m = [0^0 \quad 32^0 \quad 90^0]$. As shown in figure 6.4, the Normalized Lobe Ratio NLR = 7.6979.

Case II: The practical normalized result is obtained when, $a/\lambda = 1$, N= [1 6 12], $\theta_m = [0^0 \quad 30^0 \quad 90^0]$. The Normalized Lobe Ratio NLR =5.7. However, the NLR is relatively small w.r.t. the best normalized one, in case I.

Case III : The more practical normalized result which has a good Normalized Lobe Ratio has been obtained when, $a/\lambda = 1.1$, N= [1 6 12] and $\theta_m = [0^0 \quad 30^0 \quad 90^0]$. Figure 6.5 represents a computer generated far field pattern for SPA antenna. This figure shows the main lobe to side lobe ratio as 7.385, where the Normalized Lobe Ratio becomes better relative to case II. For this case, it is more practical one because the distances between the sources are equal in each section. The side lobe in case III is better than Case I as comparing the curves shown in figures 2.22 and 2.23. The only disadvantage in this optimization program is the long Computation time.

We have performed another optimization program on the same model using Visual C++ program (OPT-V5), we have obtained the same result, which confirm the obtained results of (OPT-M5). Here, the main advantage of (OPT-V5) is its smaller Computation time relative to that of matlab.

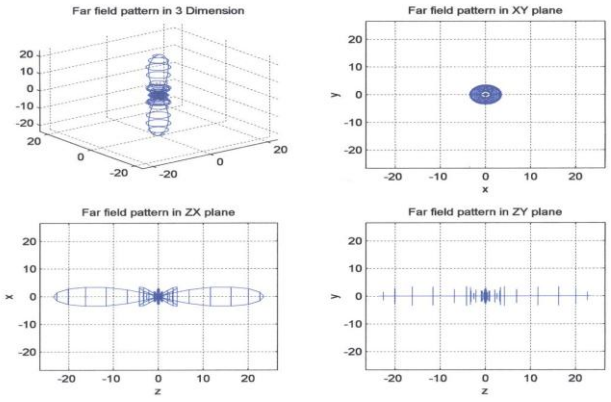

Figure 2.22, Three-dimensional antenna pattern of SPA for case I.

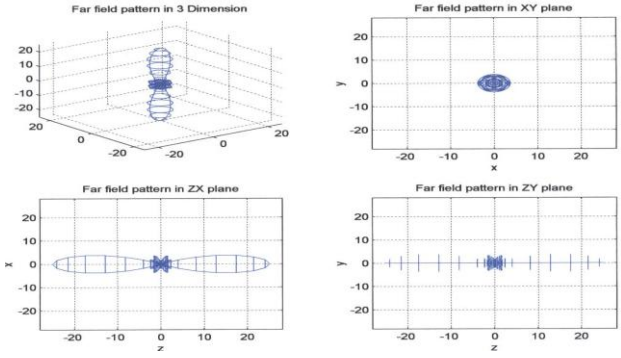

Figure 2.23, Three-dimensional antenna pattern of SPA for case III

4.2 Optimization of 7-sections for SPA antenna

By using matlab software program (OPT-M7) and Visual C++ program (OPT-V7) to optimized results for 7-sections of SPA antenna (Broad side array) by scanning parameters. The best normalized result is obtained when, $a/\lambda = 1$, N = [1 6 12 18] and $\theta_m = [\ 0^0 \quad 29^0 \quad 56^0 \quad 90^0\ ]$. As shown in figure 2.24, the Normalized Lobe Ratio is NLR = 9.2186. This case is the best normalized result and it is more practical because the distances between the sources in each section is around the same. It is noticed that the half power beamwidth is reduced relative to number of sections.

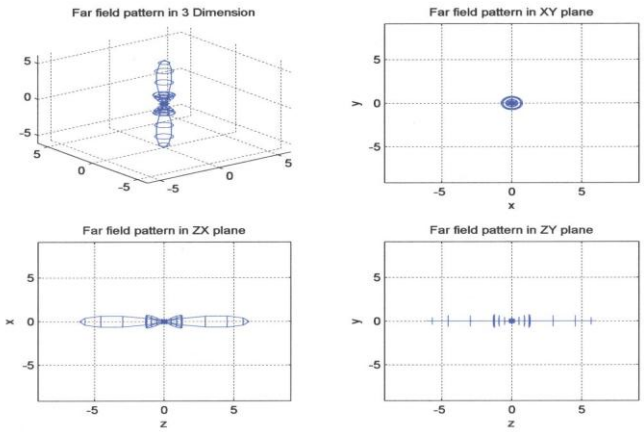

Figure 2.24, Three-dimensional antenna pattern for the optimization result of SPA for 7-sections.

4.3 Beam Steering in Spherical Phased Array Antenna of 7-sections

The maximum points can be established in any direction by applying the proper α_i to each point source. The specific values for each of the α_i can be calculated by using Equations (6-1) and letting $\psi_i = 0.$ That is to say,

$$\psi_i = ka\cos(\delta_i) + \alpha_i = 0 \qquad (1.49)$$

If the required direction in which the electric field is to have its maximum value $\boldsymbol{\theta} = \boldsymbol{\theta}_{s,}$ and $\phi = \phi_{s,}$, then the total phase shift of each source should be zero in that direction.

These are picked for demonstration purposes and other combinations are possible to steer the beam in the desired direction. The steer angles $\boldsymbol{\theta}_s$ and $\boldsymbol{\phi}_s$ were varied to exhibit the steering capability of the array.

Figure 2.25 shows the three dimensional pattern of the array factor for the 7-sections SPA when, $a/\lambda = 1$, N = [1 6 12 18], $\theta_m = [\ 0^0 \quad 29^0 \quad 56^0 \quad 90^0\ ]$ and the steering angle is on the y-axis($\theta_S = 90^0, \phi_S = 90^0$). So the characteristic of the array factor can be controlled in 3-dimension by changing the phase shifts for each point source in terms of steer angles.

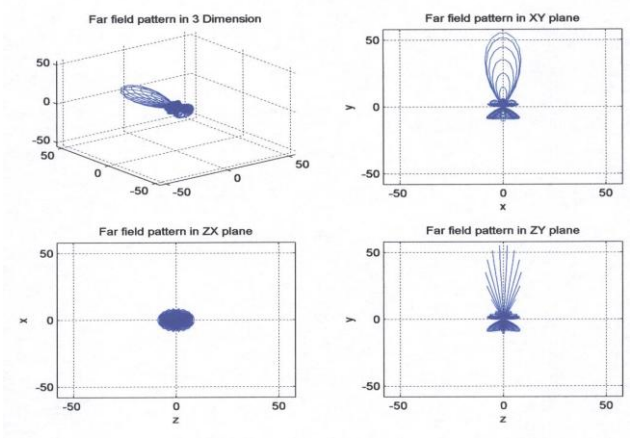

Figure 2.25, Three dimensional pattern of a SPA of 7-sections when $a/\lambda = 1$, N = [1 6 12 18], $\theta_m = [0^0 \quad 29^0 \quad 56^0 \quad 90^0]$ and equal amplitude and scanning angle $\theta_S = 90^0, \phi_S = 90^0$.

5.Conclusion And Future Work

Using the computer programs developed in this paper, several examples of antenna arrays were evaluated to determine the effecting factors on the array performance by varying one parameter each time. The following conclusion can be drawn from the analysis of the examples discussed.

5.1 Uniform and Nonuniform Amplitude Linear Array

5.1.1 Effects of Varying Number of Elements

Varying the number of elements (N) while holding displacement between elements in wavelength (d), phase shift (β) in degrees and major –to – minor lobe (Ro) in dB constant. Conclusions drawn from the plots and their calculations are:

1- If the number of elements increases the beamwidth becomes narrower.
2- There are more side lobes as N increases .
3- As the number of elements is increased further, the power is directed more in the side lobes, on the expense of the main lobe.
4- The directivity of a Dolph-Tschebyscheff array, with a given side lobe level, increases as the array size or number of elements increases.

5.1.2 Effects of Varying Displacement between Elements

Varying the displacement between the elements while the other parameters are held fixed. Conclusions drawn are:

1- The side lobe level becomes higher and the number of sidelobes increases when the displacement between the elements is increased $(0 < d < \lambda)$.
2- When the displacement is increased up to one wavelength ($d \geq \lambda$) the power is transferred from the mainbeam to the sidelobes (i.e. the sidelobes seem to become mainlobe).
3- The half-power beam width becomes bigger for decreasing displacement between elements and the directivity becomes smaller.
4- If the major-to-minor lobe ratio increases the half-power beam width becomes smaller and directivity become bigger.
5- For a given array length, or a given number of elements in the array, the directivity does not necessarily increase as the side lobe level decreases. As a matter of fact, a -15 dB side lobe array has smaller directivity than a -20dB side lobe array. This may not be the case for all other side lobe levels.

5.1.3 Effects of Varying Progressive Phase Shift

arying the progressive phase shift while the other parameters are fixed. Conclusions drawn from the plots are:
1- Reversing the phase shift (for example from 90 to -90) causes the reversal of the total radiation pattern.
2- Varying the phase shift will change the direction of the main beam and transfer the radiated power from main beam to the side lobes.

5.2 Planar Array

Through analyzing the plots the following conclusion can be written as :

5.2.1 Effects of varying Number of Elements in x- or y-axis

1-As the number of elements N in x or the number of elements M in Y increases the main beam becomes narrower.
2-There are more side lobes as N or M increases.

5.2.2 Effects of varying Displacement between Elements in x- or y-axis

Varying the displacement between elements d_x or d_y while the other parameters held fixed,
1- There are more side lobes if displacement between elements (d_x or d_y) increases.
2- When the displacement is increased up to one wavelength in x or y the power is transferred from the main beam to sidelobes.
3- The half-power beam width becomes bigger for decreasing displacement between elements and the directivity becomes smaller.

5.2.3 Effects of varying progressive phase shift

Varying the phase shift will change the direction in 3-dimensions of the main beam and transfer the radiated power from the main beam to the side lobes.

5 .3 Circular Array

5.3.1. Effects of varying number of elements

Varying the number of elements (N) while holding the radius of circular array.
1. The main to side lobe ratio increases with increasing N elements.
2. For a given radius of the circular array, if the number of elements increases furthers then the NLR and directivity does not necessarily an increase.
3. The half power beamwidth is reduced relative to number of elements.

5.3.2 Effects of varying Radius of Circular Array

Varying the radius of circular array while the other parameters are fixed.
1- When the radius of circular array increases the number of sidelobs increases.
2- For greater radius of the circular array then the number of elements must be increased.
3- As the radius of the array becomes very large the directivity of a uniform circular array approaches the value of N, where N is equal to the number of elements [3].
4- The half –power beamwidth becomes bigger for decreasing the radius of circular array.

5.3.3 Effects of varying progress phase shift.

Varying the phase shift will change the direction in 3-dimensions of the main beam and transfer the radiated power from main beam to the side lobes.

5.3.4 Spherical phased Array Antenna

Through analyzing the plots, the following conclusion can be written as :
1- The Circular Array can be brought together to form a three dimensional Spherical Phased Array (SPA).
2- Derive the general equation for Spherical phased Array (SPA) Antenna for any number of circular array sections to calculate and draw the array factor.
3- If any change in number of sections (or number of elements in each section) then the array factor will change.
4- If the radius of spherical array is less than one wavelength the Normalized Lobe Ratio becomes too small.

5- For greater radius of the spherical array then the number of sections of circular array will increase.
6- The more practical optimized result which has a good Normalized Lobe Ratio (main lobe to side lobe ratio is 7.385) has been obtained when, $a/\lambda = 1.1$, N= [1 6 12] and $\theta_m = [0^\circ \quad 30^\circ \quad 90^\circ]$, it is more practical one because the distances between the sources are equal in each section.
7- The optimized results for 7-sections of SPA antenna (Broad side array) by scanning parameters is obtained when, $a/\lambda = 1$, N = [1 6 12 18] and $\theta_m = [0^\circ \quad 29^\circ \quad 56^\circ \quad 90^\circ]$; the Normalized Lobe Ratio NLR = 9.2186. This case is the best normalized result and it is more practical because the distances between the sources in each section are around the same.
8- The half power beamwidth is reduced relative to number of sections.
9- Varying the phase shift will change the direction in 3-dimensions of the main beam and transfer the radiated power from main beam to the side lobes.

5. The Future Work in Spherical Phased Array Antenna

An array of radiating elements which lie on the surface of a sphere provides a natural antenna configuration for obtaining hemispherical coverage with nearly identical high directivity beams. This paper presents the results of an analytical study of the Spherical phased array consisting of circular array sections. Recent interest in spherical array for achieving hemispherical antenna coverage is based on the natural ability of spherical arrays to provide good uniformity of pattern and gain over wide angular regions. Other array configurations, suffer from beam degradation as the beam is steered over wide angular regions. For example, when multiple planar arrays are used to obtain hemispheric coverage, Knittel [23] has shown that at least 3 planar apertures or faces are required, and each face must be capable of steering the beam to an angle 63^0 from width broading with a gain reduction of 4.1 dB at the maximum scan angle of 63^0. This beam degradation can be reduced by using more than 3 planar faces.Cylindrical or conical arrays can reduce beam variations in azimuth, but still suffer beam variations in the elevation scan direction. When these pattern and gain variations are unacceptable, a spherical array can be used to cover the hemisphere with practically identical beams, provided the array is large in terms of wavelength.

Acknowledgements

This paper would not be complete without acknowledging Mohammed Abdullrahman Mater Almoteriy for his constant efforts made during this study

REFERENCES

[1] A.A. Oliner, G.H. Knittel, "phased array antennas", Artech House, INC. Dedham, Massachmsetts 02026.

[2] W.L. Stuzman, G.A. Theili, "Antenna theory and Design ". Johr Wiley& sons In c. 1981.

[3] Constantine A. Balanis, "Antenna theory analysis and Design. "Harper & Row, publishers, Newyork.1982, and the new addition 1997.

[4] U.R. Najib, etal "The analysis of a spherical array antenna", International Microwave Symposium Proceedings 1987,SBMO , Riode Janeiro,July 27-30,1987.

[5] R.C. Hansen , "phased array antennas",Wileyseries in microwave and optical Engineering, 1998 .

[6] Noach Amitay et al, " Theory &Analysis of Phased Array Antenna ", John Wily & Sons , Inc , 1971 .

[7] Warren L. Stutzman & Gary A. Theiele, " Antenna Theory and Design ", second edition, John Wily & Sons , Inc , 1998 .

[8] G. Aspley, L. Coltum and M. Rabinowitz," Quickly Devise a Fast Diode Phase Shifter ," Microwave, may 1979, pp 67-68.

[9] W.W. Hansen and J.R. Woodyard," A New Principle in Directional Antenna Design ," proc. IRE, VOL 26, W03, March 1938, PP.333-345.

[10] J.S. Stone, united states Patents No. 1,643,323 and No. 1,715,433, Constantine A. Balanis, "Antenna theory analysis and Design. "Harper & Row, publishers, Newyork.1982, and the new addition 1997.

[11] C.L. Dolph, " A Current Distribution for Broadside Arrays which optimizes the Relationship Between Beamwidth and side-lobe level," proc. IRE and Waves and Electrons, June 1946.

[12]M.M. Dawoud and A.P. Anderson," Design of superdirection Arrays with High Radiation Efficiency, " IEEE Trans. Antenna Propagent, VOL. A p-26. NO.6, January 1978, pp. 819-823.

[13] R.S. Elliot, " Beamwidth and Directivity of Large Scanning Arrays, " First of two parts, the Microwave Journal, December 1963, pp. 53-60.

[14] R.S. Elliot, " Beamwidth and Directivity of Large Scanning Arrays, " last of two parts, the Microwave Journal, January 1964, pp. 74-82.

[15] B.J. Forman, "A Novel Directivity Expression for planar Antenna Arrays," Radio Science, VOL.5, NO. 7, July 1970, pp. 1077-1083.

[16] James Stewart , " Calculus ", fourth edition, Brooks/Cole Publishing Company , 1999 .

[7] Eli Brookner, " Practical Phased Array Antenna Systems ",pp(3-4),(6-3), Artech House, 1991.

[18] I.J.Bahil, and P.Bahratia, " Microstrip Antennas ", Artech House, 1980.

[19] Richard C. Johnson, " Antenna Engineering Handbook ", Mcgraw-Hill,1993.

[20] J. H. provencher, "A Survey of Circular Symmetric Arrays," Polyetchnic Institute of Brooklyn Phased-Array Antenna Symposium, 1970.

[21] B. Sheleg, "A Matrix-Fed Circular Array for Continuous Scanning," Proc. IEEE, Vol.56, pp 2016-2027, November, 1968.

[22] http://www.amsjv.com/

[23] Knittel, G. H., "Choosing the Number of Faces of a Phased Array Antenna for Hemisphere Scan Coverage," IEEE Trans. Antennas and prop., Vol. AP-13, Nov. 1965, pp.878-882.

[24] Engineering Model of an Electrically Scanned Phased Array Antenna System, Final Report , Ryan Company, Report No. 59867-1, NASA/MSC Contract NAS 9-7626, May 1969.

[25] Leonidas Marantis, Erik De Witte, Paul V Brenna, "Spherical Near –Field Measurements of spherical Array Antenna'' ,Proceedings ARP '2007 The Fourth IASTED International Conference on Antennas, Radar And Wave Propagation, Page 252-258.

[26] S Pal And V Sambasiva Rao. " Spherical Phased Array Links Remote Sensors'', Microwaves And Radars, Sept 20, 2009

[27] A R Bestugin, V N Krasyuk, M B Ryzhikov." Microstrip Spherical Active Phased Array Antenna with Electronics Scanning By Means Of Rearrangement Of Patches''. Scientific Journal'' Information And Control Systems'' , ISSN 1684-8853 , Journal 4(35)/2008.

[28] Ababakhani, X Guan, A Komiljani, A Natarajan And A Hajimiri." A 77ghz 4-Element Phased Array Receiver with On chip Dipole Antenna In Silicon'', IEEE International Solid State Circuits Conference 2006.

[29] V.Sambasiva Rao, V.V. Srinivasan and S. Pal. " Generation of dual beams from spherical phased array antenna ", Electronics Letter 23 rd April 2009 Vol.45 No.9.